J Neurooncol (2014) 116:559–566
DOI 10.1007/s11060-013-1323-z

CLINICAL STUDY

Advanced MR diffusion tensor imaging and perfusion weighted imaging of intramedullary tumors and tumor like lesions in the cervicomedullary junction region and the cervical spinal cord

Xiang Liu · Wei Tian · Balasubramanya Kolar · Rui Hu · Yuqing Huang · Jason Huang · Sven Ekholm

Received: 2 July 2013 / Accepted: 15 December 2013 / Published online: 30 December 2013

Abstract Differential diagnosis between intramedullary tumors and tumor-like lesions (TLL) in the cervicomedullary junction region and cervical spinal cord is important, sometimes clinical dilemma on conventional MR imaging and empirical treatment. We evaluated advanced MR diffusion tensor imaging (DTI) and perfusion weighted imaging (PWI) in 25 patients, including 12 with intramedullary tumors and 13 with TLL in the cervicomedullary junction region and cervical spinal cord. We found that mean fractional anisotropy value of tumors was significantly lower than the value found in TLL, and the mean trace apparent diffusion coefficient and peak height values of tumors were significantly higher ($P < 0.05$). The receiver operating characteristic curve analysis showed that peak height was better than any of the other imaging parameters, with a sensitivity of 90.9 % and specificity of 80 % using a cutoff value of 4.523 to differentiate between tumors and TLL. In conclusion, the MR DTI and PWI could be useful in differentiating between intramedullary tumors and TLL in the cervicomedullary junction region and cervical spinal cord.

Keywords Diffusion tensor imaging · Perfusion weighted imaging · Intramedullary tumors · Tumor like lesions

Introduction

Intramedullary tumors and tumor-like lesions (TLL) in the cervicomedullary junction region and cervical spinal cord are sometimes difficult to distinguish between on conventional MR imaging [1–6]. Since surgical biopsy of lesions in these regions is risky procedure, it is common to treat them empirically. When correctly diagnosed, neurosurgeons can achieve a gross total resection with improved functional outcome in ~80–90 % of astrocytomas and ependymomas, which are the majority of intramedullary tumors. Recently, we reported—a case of glioblastoma in the cervical spinal cord that had been misdiagnosed as TLL based on conventional MR imaging and initial clinical treatment response [6].

MR dynamic susceptibility contrast perfusion weighted imaging (DSC-PWI) and diffusion tensor imaging (DTI) are two techniques that nowadays are commonly applied to assess the hemodynamic status and the degree of motion of water molecules in intracranial tumors, respectively [7–9]. DTI has been used to characterize cervical spinal cord tumors or multiple sclerosis plaques [10–15], but we have not found any study that compares differences in DTI metrics for these two entities. MR DSC-PWI has been proven to be useful in differentiating between cerebral tumefactive demyelinating lesions (TDLs) and high grade gliomas [16]. However, there are several technical challenges with regard to the application of DSC-PWI in the cervicomedullary junction region and the cervical spinal cord. The major challenge is the calculation of the relative cerebral blood volume (rCBV) ratio, which is the most widely used imaging index in brain DSC-PWI studies. In the brain, the rCBV ratio is defined as the CBV values of the lesion divided by the CBV value of normal appearing white matter of the contralateral hemisphere. This prerequisite, however, may be invalid in the analysis of DSC-PWI examinations in the cervicomedullary junction/cervical spinal cord as intramedullary lesions here can involve most of the medulla/cord resulting in inaccurate ratio measurements.

X. Liu (✉) · W. Tian · B. Kolar · R. Hu · Y. Huang · J. Huang · S. Ekholm
University of Rochester, Rochester, NY, USA
e-mail: xiang_liu@urmc.rochester.edu

Cha et al. [17] introduced two hemodynamic variables derived from MRDSC-PWI (the peak height and the percentage of signal intensity recovery) that may provide additional information on tumor vascularity. These two parameters are derived directly from the time-signal intensity curve obtained within the lesion by DSC-PWI and there is thus no need for contralateral reference tissue information. In our previous preliminary study, we found that the peak height correlated with the rCBV ratio in non-enhancing gliomas and non-neoplastic lesions in the cervicomedullary junction region, which suggests that this index might also be useful in differentiating between such lesions in the cervicomedullary junction region [18]. We decided to assess the value of the peak height and the percentage of signal intensity recovery for DSC-PWI as well as trace apparent diffusion coefficient (ADC) and fractional anisotropy (FA) derived from DTI in differentiating between contrast enhancing intramedullary tumors and TLLs in the cervical spinal cord and the cervicomedullary junction region.

Materials and methods

We retrospectively analyzed data acquired as part of an Institutional Review Board—approved, Health Insurance Portability and Accountability compliant study. The need to obtain informed consent was waived. MRI examinations of 25 patients (10 female, 15 male) were reviewed, including 12 patients (mean age 25 ± 22 years old) with tumors, and 13 patients (mean age 42 ± 12 years old) with TLLs. There were 23 patients with DTI examinations (11 with tumors and 12 with TLLs), and 21 patients with PWI examinations (11 with tumors and 10 with TLLs).

All tumors were confirmed by histopathologic examination of tissue obtained by biopsy, surgical resection or at autopsy. The tumors included astrocytoma, ependymoma, and glioblastoma. The patient with glioblastoma had been partially described in our previous case report [6]. The TLL cases were diagnosed by clinical follow-up and supportive laboratory testing. Clinically, these patients had a history of multiple sclerosis, transverse myelitis, or sarcoidosis. They had an acute to subacute onset of signs or symptoms involving a focal neurologic deficit mimicking findings of intramedullary tumors. Patients had no evidence of systemic illness, malignancy, or immunosuppression [18]. None of the patients had steroid treatment at the time of imaging. All patients with TLL had follow-up MR imaging examinations within 4–12 months after the initial examination and these follow-up examinations showed either regressing or stable lesion.

MR examinations were performed on either 1.5 or 3 T MR imaging system (GE Medical Systems, Milwaukee, WI, USA). Except DTI and PWI examinations in five cases with tumor like lesions examinations were performed in the 3 T scanner, MR examinations of other patients with tumor like lesions and tumors were acquired on 1.5 T MR scanner. The DTI protocol included sagittal and axial acquisitions (TR/TE = 12,000/101.7 ms, with a FOV = 23 × 23 cm^2 for the sagittal sequence and 17 × 17 cm^2 for axial acquisition. Matrix = 128 × 128, thickness = 4 mm and gap = 0 mm using 25 noncollinear gradient directions and a b value of 1,000 s/mm^2. Another three images were acquired without the use of a diffusion gradient, b = 0 s/mm^2). The acquisition time was approximately 3 min for the sagittal plane and 6 min for the axial. The DSC-PWI images were acquired with a single-shot, gradient-echo, echo-planar imaging sequence (TR/TE = 1,500/50 ms; flip angle, 80°; FOV = 17 × 17 cm^2 in 20 cases and 23 × 23 cm^2 in one case of glioblastoma; matrix = 96 × 128; thickness = 5 mm and gap = 0 mm.) during the first pass of a bolus of gadoversetamide. The amount of contrast agent injected was 0.1 mmol per kilogram of body weight, maximum 20 mL (1.5 T) and 0.05 mmol/kg of body weight (11), maximum 12 mL (3 T). The total dose was injected in 4 s (1.5 T) and 3 s (3 T), respectively, immediately followed by a bolus injection of saline (20 mL) [18]. The spatial localization of the slice with largest dimension in PWI, DTI and the corresponding post contrast T1 weighted imaging sequence was carefully kept to be identified.

MR-DTI data were processed on a GE workstation with a Functool 5.2 software package. After co-registration of raw images to correct the motion and distortion artifacts, the ADC and FA images were generated. The solid parts of the lesions were delineated and regions of interest (ROIs) of ~23–28 mm^2 each were placed in the center of the solid part of the lesion, while the necrotic parts were avoided.

The DSC-PWI data analysis was described in a previous study [18]. In brief, a ROI of ~23–35 mm^2 was placed within the solid central part of the lesion at the slice with largest dimension. The signal-intensity curves of the lesion ROIs' were converted to R2* curves based on the formula: $R2^* = -\ln(S_t/S_0)/TE$, where ln is the natural log and S_t and S_0 are signal intensities at time t and 0 [17–19]. The first four images were excluded as they were acquired during the time the steady-state MR signal was established. The peak height was calculated as the formula: peak height = $height_m - height_b$, (the $height_m$ is maximal height during the bolus phase of the first pass of contrast minus the height of precontrast baseline, and the $height_b$ means the height of precontrast baseline). The percentage of signal intensity recovery was calculated with the following equation: percentage of signal intensity recovery = maximal height − $height_b$/maximal height − $height_e$, ($height_e$ indicates the height at the end of the first pass).

In addition, reference ROIs in the contralateral/surrounding normal appearing medulla/cord were selected in order to compare the difference of FA, ADC and peak height between the lesions and reference tissue. The references ROIs, ~20–35 mm^2 each, were defined as follows:

1. For patients with ipsilateral (eccentric) lesions, the reference ROIs were selected in the contralateral normal appearing medulla/cord (15/23 DTI examinations, 13/21 PWI examinations);
2. For patients with central lesions, and a normal-appearing adjacent portion of the cord (no signs of expansion or atrophy and normal signal intensity on T1 and T2WI) in the same slice, reference ROIs were placed in the adjacent tissue (4/23 DTI examinations, 6/21 PWI examinations);
3. For patients with central lesions and where the adjacent part of the cord showed hyperintensity on T2WI, or patients with ipsilateral (eccentric) lesions, where the contralateral medulla/cord showed hyperintensity on T2WI, the normal appearing tissue in the slice closest to the lesions was selected for a reference ROI (4/23 DTI examinations, 2/21 PWI examinations);

Finally, values of FA, ADC, peak height and the percentage of signal intensity recovery in remote normal-appearing cord or medulla regions were measured.

The statistical analyses included five parts. First, the differences in FA, ADC and peak height between the lesions and the reference ROIs were assessed by Wilcoxon signed-rank test. Second, comparisons of FA, ADC, the percentage of signal intensity recovery and peak height between the intramedullary tumor group and the TLL group were performed by Mann–Whitney test. Then, the area under the curve (AUC) for receiver operating characteristics (ROC) was computed for ADC, FA, percentage of signal intensity recovery and peak height, respectively. The difference of FA, ADC, peak height and the percentage of signal intensity recovery values in remote normal-appearing cord or medulla regions among patients with tumor like lesions who were scanned on 1.5 and 3 T scanners, and the group of patients with tumors scanned on 1.5 T was evaluated with Mann–Whitney test. Finally, Spearman correlation analysis was used to assess the correlation between changes of FA and ADC within the lesions. Statistical analyses were performed with SPSS for Windows software (version 15, SPSS Inc., Chicago, IL, USA) and R (A Language and Environment for Statistical Computing, Vienna, Austria, http://www.R-project.org) with P values of <0.05 recognized as the criteria for significance.

Results

The mean values of imaging parameters and the statistical results are shown in Table 1. When compared with the mean FA values of the reference ROIs, the mean FA values of the tumors and TLLs were significantly lower ($P < 0.05$, representative image in Fig. 1). There is only one case of a solitary astrocytoma which had higher FA value within the tumor than in the perilesional region. This finding was confirmed on a repeat DTI examination (Fig. 2).

The mean ADC values in the tumors and TLLs were significantly higher compared to reference ROIs ($P < 0.05$).

The mean value of peak height in the tumors was significantly higher than the value of reference ROIs, Fig. 3. In contrast, the mean value of peak height in the TLLs was significantly lower than the value of reference ROIs ($P < 0.05$), Fig. 4.

The mean peak height and ADC values of the tumors were significantly higher than those of the TLLs, while the mean FA value of the tumors was significantly lower ($P < 0.05$). There was no significant difference with regard to percentage of signal intensity recovery between the two groups.

Table 1 Mean values (mean ± SD) and statistical result of imaging parameters in patients with tumors and tumor like lesions

Imaging parameters		Tumors	TLLs	P
FA	In the lesion	0.232 ± 0.076	0.39 ± 0.111	0.002*
	Reference ROI	0.386 ± 0.093	0.627 ± 0.11	$P < 0.001$*
	P value	0.003*	0.003*	N/A
ADC ($\times 10^{-3} mm^2/s$)	In the lesion	1.285 ± 0.505	0.862 ± 0.166	0.016*
	Reference ROI	0.844 ± 0.339	0.747 ± 0.117	0.525
	P value	0.002*	0.006*	N/A
Peak height	In the lesion	15.167 ± 9.05	3.906 ± 1.747	$P < 0.001$*
	Reference ROI	8.99 ± 5.134	6.872 ± 2.23	0.973
	P value	0.003*	0.005*	N/A
Percentage of signal intensity recovery		0.83 ± 0.34	0.87 ± 0.23	0.512

* indicates statistical significance

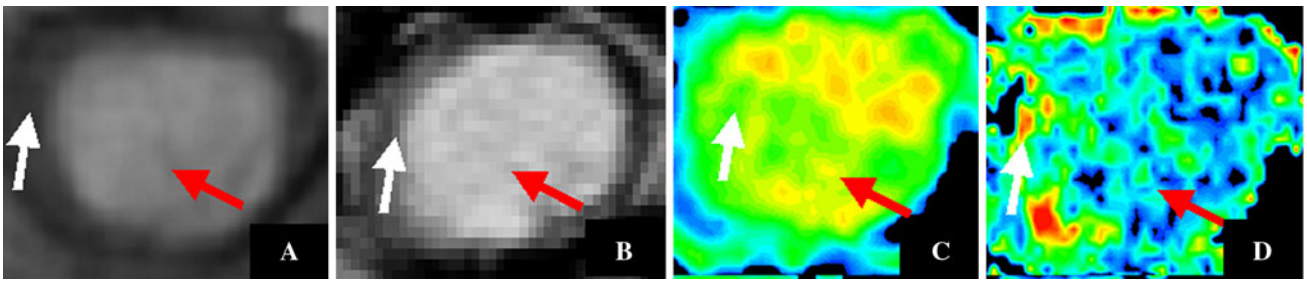

Fig. 1 A case of astrocytoma with reduced FA value in the tumor. **a**–**d** are at the C2–3 level. **a** Axial T1-weighted post-contrast image shows the enhancing solid part of tumor (*red arrow*), and adjacent compressed cord (*white arrow*). **b** Axial T2-weighted image shows hyperintensiy in the tumor (*red arrow*), and iso-intensity and slightly hyperintensiy in the adjacent cord (*white arrow*). **c** ADC map shows increased ADC in both parts of the tumor (*red arrow*) compared to adjacent cord (*white arrow*). **d** FA map shows decreased FA value within solid part of tumor (*red arrow*) of 0.283, compared to adjacent cord (*white arrow*) of 0.427

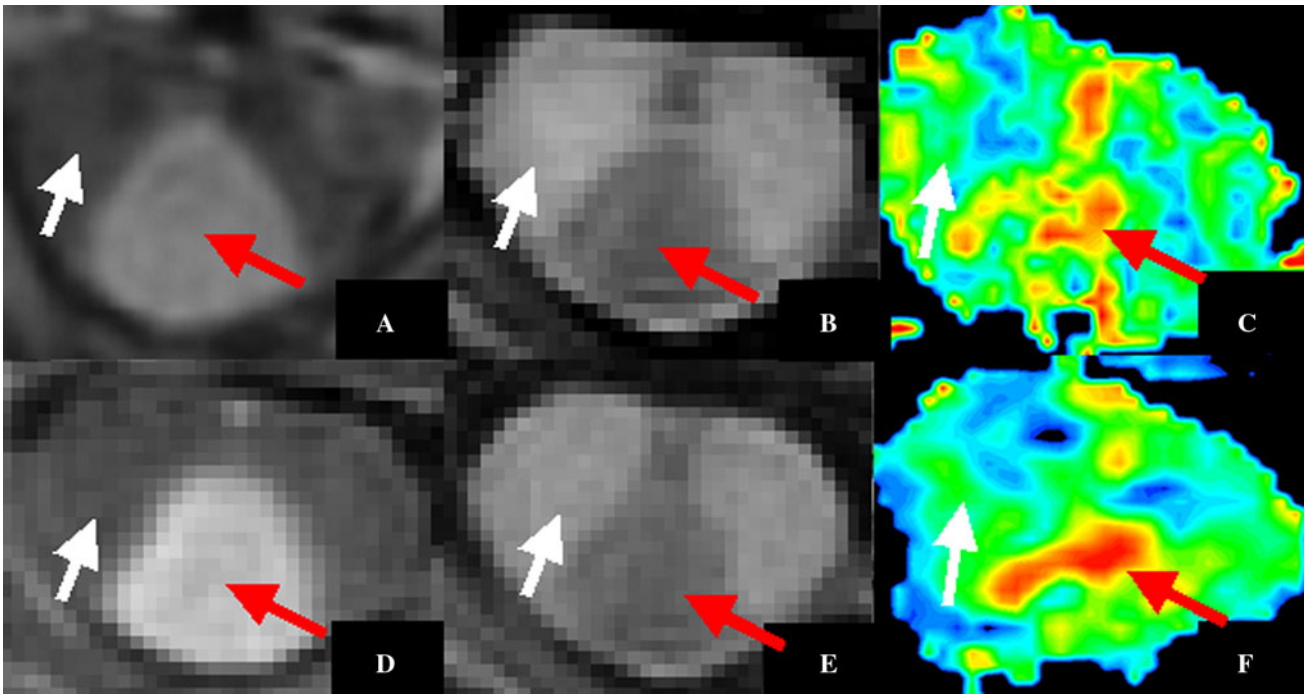

Fig. 2 A patient with astrocytoma with "increased" FA value in the tumor. **a**, **d** Axial T1-weighted post-contrast images; **b**, **e** T2-weighted images; **c**, **f** FA images. **a**–**c**: Images from first examination, which show the FA value in the enhanced tumor part (0.336) to be higher than in the adjacent cord (0.159). **d-f**: Follow-up images 1 year later after radiation treatment, which show the contrast enhanced area to be decreased but the FA value in the enhanced part of the tumor (0.28) still being higher than in the adjacent cord (0.136)

The sensitivity and specificity of the imaging parameters to distinguish between intramedullary tumors and TLLs, using ROC curve analysis, are summarized in Table 2. The ratio cutoff value of 4.523 for peak height resulted in a sensitivity of 90.9 % and a specificity of 80 %. The area under the curve for peak height was higher than FA and ADC.

There was no significant difference of FA, ADC, peak height and the percentage of signal intensity recovery values in remote normal-appearing cord or medulla regions among patients with tumor like lesions who were scanned on 1.5 and 3 T scanners, and the group of patients with tumors scanned on 1.5T ($P > 0.05$).

There was no significant correlation between FA and ADC value in patients with tumor like lesions ($P = 0.247$), however, there was significant negative correlation between FA and ADC value in patients with tumors ($P = 0.021$).

Discussion

In the present study, there were three parameters, ADC, FA and peak height, that showed a significant difference between tumors and TLL. The peak height of the bolus passage showed higher sensitivity and specificity than all

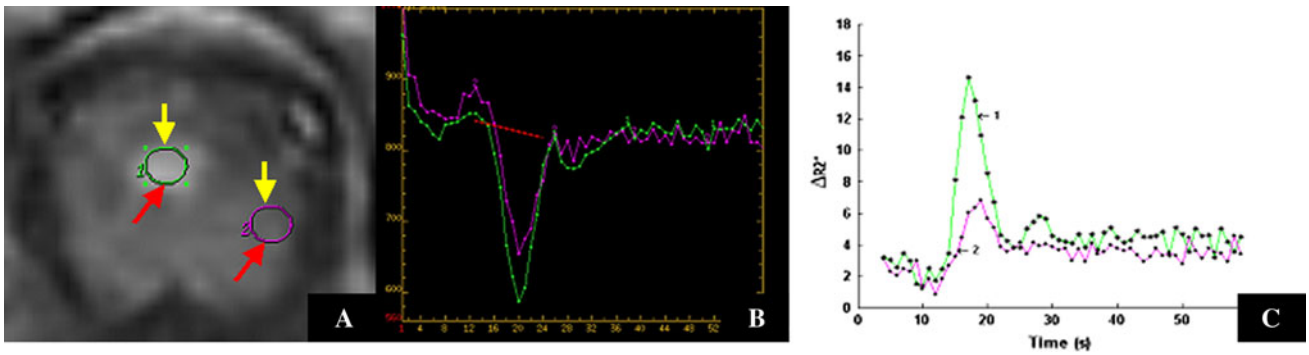

Fig. 3 A patient with astrocytoma in medulla. **a** Axial T1-weighted post contrast image shows: ROI 1 (*green*) placed in the contrast enhanced solid part of the tumor, ROI 2 (*purple*) located in the contralateral medulla as reference. **b** The time-signal intensity curves of ROIs. **c** The ΔR2 curves show that the peak height of the tumor (12.9024) is significantly higher than the peak height of reference ROI (5.9726)

Table 2 Sensitivity and specificity of imaging parameters in the differentiation of intramedullary tumors and tumor like lesions using receiver operating characteristic curve analysis

Parameters	Cutoff value	Sensitivity	Specificity	AUC
FA	0.272	0.75	0.727	0.871
ADC	0.969	0.75	0.818	0.795
Peak height (PWI)	4.523	0.909	0.8	0.945
Percentage SIR	0.861	0.545	0.5	0.591

AUC area under curve, *SIR* signal intensity recovery (PWI)

the other imaging parameters tested. In addition, the mean FA values in both intramedullary tumors and TLLs were significantly lower compared to values in the reference ROIs, and the mean values of ADC in both tumors and TLL were significantly higher than the values of reference ROIs.

The anatomic feature of cervical spinal cord is characterized by the densely ordered arrangement of axons [20]. Thus, lesions in the cord may have a lower FA value than normal cord parenchyma [10, 11], which was also noted in our study. In earlier studies, Ducreux et al. [10] reported a mean FA value of 0.48 ± 0.02 in five cases of cervical spinal cord astrocytoma and Renoux et al. [11] demonstrated a mean FA value of 0.588 in inflammatory lesions. The mean FA values of tumor and tumor like lesions in the present study are 0.232 ± 0.07 and 0.39 ± 0.111, respectively, which are lower than the findings in previous studies [10, 11]. The differences may relate to the following:

(1) The study of Ducreux et al. [10] represented pure astrocytomas while there is a variability of tumor types enrolled in the present study, also including glioblastoma and ependymoma. These tumors may cause more severe tissue destruction than the more prominent infiltration by astrocytomas.
(2) There are differences in measurement techniques. In previous studies, small ROIs were placed in the lesions while we measured the mean diffusion values of the gross solid portion of the lesions.
(3) We can't exclude that the differences are a result of imaging parameters, especially the lower b-value of 500 s/mm^2 used in Ducreux's study [10] and of 600 s/mm^2 used in Renoux's study [11] as compared to 1,000 s/mm^2 in the present study. The mean FA value of TLLs in our study coincides with the study by Ohgiya et al. [15] who also used a *b*-value of 1,000 s/mm2 with a reported mean FA value of 0.441 ± 0.070 in multiple sclerosis plaques of the cervical spinal cord.

The pathologic mechanisms behind the decrease in FA are supposed to be related to an increase in extracellular space with a corresponding decrease in the intracellular space [10, 11]. Both tumors and TLLs can present decreased FA as a result of local extracellular edema and/or a decrease in number of fibers. Moreover, both infiltration and displacement of fibers by tumors as well as reduction in myelin content, as in multiple sclerosis, can result in a decrease in FA.

In this present study, except one case with astrocytoma, other tumors and all tumor-like lesions had lower FA values within the lesion than in the reference ROIs, and we found significant negative correlation between FA and ADC value in the patients with tumors. In theory, the pathogeneses, induced decrease in FA can be caused by changes in water content and result in reduced restriction of water motion within the lesion, which could subsequently lead to increase in ADC. However, the association between quantitative changes of FA and ADC within the lesions of central nervous system may be complex. The present study showed significantly increased ADC and decreased FA values in tumors when compared to tumor like lesions, which may indicate a more severe destruction of the normal structures by the tumors and FA may be more sensitive than ADC in detecting microstructure abnormality. Our

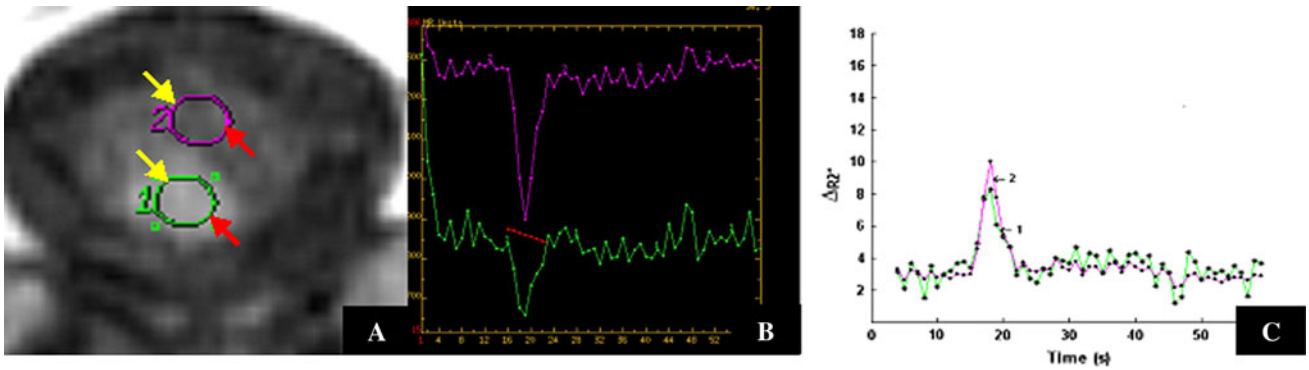

Fig. 4 A patient with multiple sclerosis in C2 cord. **a** Axial T1-weighted post-contrast image shows an enhancing lesion in the dorsal cord at C2 level. ROI 1 (*green*) placed within the contrast enhanced lesion, ROI 2 (*purple*) located in the anterior cord as reference. **b** The time-signal intensity curves of ROIs. **c** The ΔR2 *curves* show that the peak height of the contrast enhanced multiple sclerosis lesion (4.8239) is significantly lower than the peak height of reference ROI (7.0589), and peak height of astrocytoma in Fig. 3c (12.9024)

previous study reported that sub-acute Wallerian degeneration after brain stroke could show decreased ADC and FA value in the ipsilateral cortical spinal tract [21]. In addition, the present study also revealed one astrocytoma case with higher intra-tumor FA value than reference ROIs.

The mechanism of higher FA value in the exceptive astrocytoma case remains unclear. Renoux et al. [11] described higher FA value within demyelinating lesion in the cord than the reference ROIs. This increase in FA values was believed to represent intracellular edema with inflow of extracellular water into axons or Schwann cells, or alternatively decreased extracellular space due to cellular infiltration by inflammatory cells [11]. In contrast, there is no study reporting "increased" FA values within intramedullary tumors. We believe this relates to the predominantly infiltrative growth of astrocytoma cells along fibers within the cord and/or that the tumor encompasses the fiber tracts.

The peak height of the contrast bolus has been reported to correlate with rCBV and the total capillary volume in brain tumors [17, 18]. In the present study, there was a significantly higher peak height value in the intramedullary tumors than in TLLs, which is similar to an earlier study of cerebral lesions that showed a higher rCBV ratio in cerebral gliomas than in TDL [16]. Absence of frank angiogenesis and hypoperfusion secondary to decreased metabolic demand in TLL, including multiple sclerosis, have been attributed to this difference [14, 16]. Our study also demonstrated a higher sensitivity of 90.9 % and specificity of 80 % for the peak height of the bolus passage than other imaging parameters in differentiating between intramedullary tumors and TLL.

The difficulties for MR DTI and PWI of intramedullary lesions in the cervicomedullary junction region and cervical spinal cord include the intrinsic susceptibility artifacts and image distortion from the echo-planar sequence, chemical-shift artifacts from surrounding lipids, motion artifacts and partial volume effects from cerebrospinal fluid [6, 18, 22].

There are also other technical challenges including controversies in the selection of axial or sagittal orientation as the acquisition plane. Traditionally, axial plane is most commonly used for cerebral PWI and DTI acquisitions, and ROIs can be placed in the parenchyma of the unaffected hemisphere for calculation of ratios, including rCBV ratio. However, intramedullary lesions in the cervicomedullary junction region and cervical spinal cord may affect multiple segments and also involve the medulla/cord on both sides. Thus, axial plane acquisition may not cover the whole lesion and reference ROIs placed in an adjacent, perilesional part of the medulla/cord can't exclude an underestimation of pathologic changes. The sagittal plane may be an alternative approach for DTI and DSCPWI acquisition in the cervicomedullary junction region and cervical spinal cord. Potential advantages of the sagittal acquisition plane include the ability to cover the entire lesion and the possibility of using the cerebellum for the placement of a reference ROI, future studies using advanced MR imaging sequences, including parallel imaging and trigger techniques, may improve the image quality [6, 22].

It is also interesting that whether there is difference of DTI and PWI examinations in the cervicomedullary junction region and cervical spinal cord between 1.5 and 3 T MR scanners. Our preliminary study showed that there was no significant quantitative difference of FA, ADC, peak height and the percentage of signal intensity recovery in remote normal appearing tissues between 1.5 and 3 T MR scanners. In theory, a 3 T MR scanner should have more advantages, including better signal to noise ratio when compared to 1.5 T MR scanner, but may also induce more inhomogeneity artifacts [22, 23]. There is controversy regarding whether there is difference of quantitative DTI evaluation between 1.5 and 3 T MR scanners in the

literature [24–27], most of studies didn't find significant quantitative difference of FA and ADC between 1.5 and 3 T MR scanners [24–26]. This is consistent with our previous DTI study in brain glioma [28]. In contrast, there was no published study directly comparing quantitative PWI derived parameters between 1.5 and 3 T MR scanners. The peak height and the percentage of signal intensity recovery were not only determined by intrinsically pathologic characters, but also can be affected by the factors including magnetic field, and bolus dose, etc. Previous published studies showed that peak height could correlate with rCBV ratio in both 1.5 and 3 T MR scanners [17, 18]. Future perspective study with larger population is necessary to assess the qualitative and quantitative difference of DTI and PWI examinations in the cervicomedullary junction region and the cervical spinal cord.

In summary, the present study showed a significantly higher peak height and ADC, as well as lower FA in the intramedullary tumors than the TLLs. The peak height had the highest sensitivity and specificity among the three, but a combination of DTI and PWI parameters may strengthen the diagnostic accuracy with regard to intra-axial tumors and TLL in the cervicomedullary junction region and cervical spinal cord. Although preliminary, these findings may allow for a restraint with regard to immediate invasive biopsy procedures, and could support therapeutic decision making as well as monitor treatment response in future studies.

Conflict of interest The authors declare that they have no conflict of interest.

Ethical standards This is an Institutional Review Board—approved, Health Insurance Portability and Accountability compliant study. The need to obtain informed consent was waived.

References

1. Chimelli L (2001) Tumors and tumor like lesions of the spine and spinal cord. Neuroimaging Clin N Am 11:79–110
2. Van Goethem JW, van den Hauwe L, Ozsarlak O et al (2004) Spinal tumors. Eur J Radiol 50:159–176
3. Waziri A, Vonsattel JP, Kaiser MG et al (2007) Expansile, enhancing cervical cord lesion with an associated syrinx secondary to demyelination. Case report and review of the literature. J Neurosurg Spine 6:52–56
4. Dohi N, Ishikawa S, Kamijyo Y et al (2003) Multiple sclerosis with open-ring enhancement in the cerebrum and spinal cord. Intern Med 42:273–276
5. Braverman DL, Lachmann EA, Tunkel R et al (1997) Multiple sclerosis presenting as a spinal cord tumor. Arch Phys Med Rehabil 78:1274–1276
6. Liu X, Germin BI, Ekholm S (2011) A case of cervical spinal cord glioblastoma diagnosed with MR diffusion tensor and perfusion imaging. J Neuroimaging 21:292–296
7. Law M, Yang S, Wang H et al (2003) Glioma grading: sensitivity, specificity, and predictive values of perfusion MR imaging and proton MR spectroscopic imaging compared with conventional MR imaging. Am J Neuroradiol 24:1989–1998
8. Wang S, Kim S, Chawla S et al (2009) Differentiation between glioblastomas and solitary brain metastases using diffusion tensor imaging. Neuroimage 44:653–660
9. Kinoshita M, Hashimoto N, Goto T et al (2008) Fractional anisotropy and tumor cell density of the tumor core show positive correlation in diffusion tensor magnetic resonance imaging of malignant brain tumors. Neuroimage 43:29–35
10. Ducreux D, Lepeintre JF, Fillard P et al (2006) MR diffusion tensor imaging and fiber tracking in 5 spinal cord astrocytomas. Am J Neuroradiol 27:214–216
11. Renoux J, Facon D, Fillard P et al (2006) MR diffusion tensor imaging and fiber tracking in inflammatory diseases of the spinal cord. Am J Neuroradiol 27:1947–1951
12. Agosta F, Benedetti B, Rocca MA et al (2005) Quantification of cervical cord pathology in primary progressive MS using diffusion tensor MRI. Neurology 64:631–635
13. Valsasina P, Rocca MA, Agosta F et al (2005) Mean diffusivity and fractional anisotropy histogram analysis of the cervical cord in MS patients. Neuroimage 26:822–828
14. Hesseltine SM, Law M, Babb J et al (2006) Diffusion tensor imaging in multiple sclerosis: assessment of regional differences in the axial plane within normal-appearing cervical spinal cord. Am J Neuroradiol 27:1189–1193
15. Ohgiya Y, Oka M, Hiwatashi A et al (2007) Diffusion tensor MR imaging of the cervical spinal cord in patients with multiple sclerosis. Eur Radiol 17:2499–2504
16. Cha S, Pierce S, Knopp EA et al (2001) Dynamic contrast-enhanced T2*-weighted MR imaging of tumefactive demyelinating lesions. Am J Neuroradiol 22:1109–1116
17. Cha S, Lupo JM, Chen MH et al (2007) Differentiation of glioblastoma multiforme and single brain metastasis by peak height and percentage of signal intensity recovery derived from dynamic susceptibility-weighted contrast-enhanced perfusion MR imaging. Am J Neuroradiol 28:1078–1084
18. Liu X, Kolar B, Tian W et al (2011) MR perfusion weighted imaging may help in differentiating between non-enhancing gliomas and non-neoplastic lesions in the cervicomedullary junction. J Magn Reson Imaging 34:196–202
19. Maeda M, Yuh WT, Ueda T et al (1999) Severe occlusive carotid artery disease: hemodynamic assessment by MR perfusion imaging in symptomatic patients. Am J Neuroradiol 20:43–51
20. Cercignani M, Horsfield MA, Agosta F et al (2003) Sensitivity-encoded diffusion tensor MR imaging of the cervical cord. Am J Neuroradiol 24:1254–1256
21. Liu X, Tian W, Li L, Kolar B et al (2012) Hyperintensity on diffusion weighted image along ipsilateral cortical spinal tract after cerebral ischemic stroke: a diffusion tensor analysis. Eur J Radiol 81:292–297
22. Maier SE, Mamata H (2005) Diffusion tensor imaging of the spinal cord. Ann NY Acad Sci 1064:50–60
23. Alvarez-Linera J (2008) 3 T MRI: advances in brain imaging. Eur J Radiol 67:415–426
24. Hunsche S, Moseley ME, Stoeter P, Hedehus M (2001) Diffusion-tensor MR imaging at 1.5 and 3.0 T: initial observations. Radiology 221:550–556
25. Alexander AL, Lee JE, Wu YC, Field AS (2006) Comparison of diffusion tensor imaging measurements at 3.0 T versus 1.5 T with and without parallel imaging. Neuroimaging Clin N Am 16:299–309
26. Moser MJ, Breger RK, Khatri BO, Liu Y (2009) Comparison of 1.5 and 3.0 Tesla MRI diffusion tensor imaging (DTI) in patients with multiple sclerosis. Proc Intl Soc Mag Reson Med 17:1155

27. Fushimi Y, Miki Y, Okada T et al (2007) Fractional anisotropy and mean diffusivity: comparison between 3.0-T and 1.5-T diffusion tensor imaging with parallel imaging using histogram and region of interest analysis. NMR Biomed 20:743–748

28. Liu X, Tian W, Kolar B et al (2011) MR diffusion tensor and perfusion weighted imaging in preoperative grading of supratentorial non-enhancing gliomas. Neuro-Oncology 13: 447–455